




USP35 dimer prevents its degradation by E3 ligase CHIP through auto-deubiquitinating activity

Jinyoung Park^{1,2} · Sang Chul Shin³ · Kyeong Sik Jin⁴ · Min Joon Lim⁵ · Yeojin Kim^{1,6} · Eunice EunKyeong Kim⁵ · Eun Joo Song⁷ 

Received: 14 November 2022 / Revised: 23 February 2023 / Accepted: 1 March 2023 / Published online: 1 April 2023
© The Author(s), under exclusive licence to Springer Nature Switzerland AG 2023

Abstract

Recently, a number of reports on the importance of USP35 in cancer have been published. However, very little is known about the exact mechanism by which USP35 activity is regulated. Here, we show the possible regulation of USP35 activity and the structural specificity affecting its function by analyzing various fragments of USP35. Interestingly, the catalytic domain of USP35 alone does not exhibit deubiquitinating activity; in contrast, the C-terminal domain and insertion region in the catalytic domain is required for full USP35 activity. Additionally, through its C-terminal domain, USP35 forms a homodimer that prevents USP35 degradation. CHIP bound to HSP90 interacts with and ubiquitinates USP35. However, when fully functional USP35 undergoes auto-deubiquitination, which attenuates CHIP-mediated ubiquitination. Finally, USP35 dimer is required for deubiquitination of the substrate Aurora B and regulation of faithful mitotic progression. The properties of USP35 identified in this study are a unique homodimer structure, regulation of deubiquitinating activity through this, and utilization of a novel E3 ligase involved in USP35 auto-deubiquitination, which adds another complexity to the regulation of deubiquitinating enzymes.

Keywords USP35 · Auto-deubiquitination · Homodimer · CHIP · HSP90

✉ Eunice EunKyeong Kim
eunice@kist.re.kr

✉ Eun Joo Song
esong@ewha.ac.kr

- ¹ Biomedical Research Division, Center for Advanced Biomolecular Recognition, Korea Institute of Science and Technology (KIST), Seoul 02792, Korea
- ² Division of Bio-Medical Science and Technology, KIST-School, University of Science and Technology (UST), Seoul 02792, Korea
- ³ Research Resources Division, Technological Convergence Center, Korea Institute of Science and Technology (KIST), Seoul 02792, Korea
- ⁴ Pohang Accelerator Laboratory, Pohang University of Science and Technology, Pohang 37673, Kyungbuk, Korea
- ⁵ Biomedical Research Division, Medicinal Materials Research Center, Korea Institute of Science and Technology (KIST), Seoul 02792, Korea
- ⁶ Department of Life Sciences, College of Life Sciences and Biotechnology, Korea University, Seoul 02841, Korea
- ⁷ Graduate School of Pharmaceutical Sciences, College of Pharmacy, Ewha Womans University, Seoul 03760, Korea

Introduction

Ubiquitin-specific protease 35 (USP35) plays a role in a variety of cellular functions such as mitophagy [1], endoplasmic reticulum (ER) stress [2], mitosis [3], and ciliopathies [4]. Additionally, the roles it plays in cancer attracted attention. Higher USP35 expression in estrogen receptor α positive (ER α +) breast cancer is associated with accelerated cell proliferation. USP35 enhances ER α stability by deubiquitinating ER α and increases the transcriptional activity of ER α , the nuclear translocation of which is mediated through phosphorylation by AKT in ER α + breast cancer [5]. USP35 is also upregulated in ovarian cancer and has been correlated with reduced CD8+ T-cell infiltration. Mechanistically, USP35 directly deubiquitinates and inactivates STING, suppressing the activation of the STING-TBK1-IRF3 pathway and the expression of type I interferons, subsequently regulating cisplatin sensitivity in ovarian cancer [6]. In addition, USP35 has been reported to be involved in ER stress-induced apoptosis via targeting RRBPI [7], cisplatin-induced apoptosis by stabilizing BIRC3 [8], and ferroptosis by interacting with ferroportin [9] in lung cancer.

These findings suggest that USP35 might be a promising therapeutic target to overcome cancer. However, the regulation of USP35 activity and the relationship between structure and function are poorly understood.

Diverse cellular mechanisms regulate the activity of deubiquitinating enzymes (DUBs). These mechanisms include subcellular localization, post-translational modification (PTM), and protein–protein interaction. In addition, the full catalytic activity of a DUB does not rely solely on the catalytic domain; in contrast, the action of its non-catalytic domains is required. For example, in USP7, the two UBL domains in the C-terminus necessarily interact with the switching loop in the catalytic domain, which promotes the binding of ubiquitin and increases USP7 activity [10]. Similarly, to achieve its full catalytic activity, USP4 requires the N-terminal DUSP-UBL domain, which promotes changes in the switching loop by enhancing ubiquitin dissociation, resulting in the efficient control of activity [11]. Additionally, conformational changes mediated through oligomerization can determine whether a DUB is in an active or inactive state. Liu and colleagues have shown that USP25, which contains a long insertion in the catalytic domain, establishes homotetrameric form through the assembly of two dimers. Strikingly, the USP25 dimer shows higher activity, whereas the USP25 tetramer loses DUB activity, which eventually affects the stabilization of substrate tankyrases [12]. USP28 comprises a domain architecture identical to that of USP25, but USP28 forms only a dimer, not a tetramer, and exhibits completely different functions compared to those of USP25 [13, 14]. Sometimes, interaction with non-substrate partners is required for the full catalytic activity of a DUB. These partners can affect the enzymatic activity of a DUB by driving PTMs such as ubiquitination [15]. The ubiquitination of Ataxin-3 at the Lys117 residue facilitates its enzymatic activity, leading to aggresome formation [16]. In contrast, monoubiquitination of UCH-L1 inhibits the binding of ubiquitinated target proteins, inhibiting enzyme activity. However, this modification is reversed by auto-deubiquitination mediated by UCH-L1 [17].

Similar to UCH-L1, other DUBs exhibit auto-regulatory deubiquitination mechanisms that depend on their catalytic activity. For example, the inactive form of USP4 or the catalytic domain of USP4 alone (which does not show full activity) establishes enhanced covalent binding of ubiquitin compared with that of the wild-type protein, indicating that USP4 ubiquitination is prone to turnover, which is related to its catalytic activity [18]. The ubiquitin-conjugating enzyme UBE2O catalyzes monoubiquitination of multiple BAP1 residues, promoting its cytoplasmic localization. BAP1 auto-deubiquitination through intramolecular interactions

counteracts this monoubiquitination and allows BAP1 to function as a tumor suppressor [19]. In addition, USP7 [20] and USP19 [21] have been reported to remove ubiquitin that had been attached to themselves through their enzymatic activity.

In this study, we show that USP35 engages in homodimeric interactions via its highly conserved C-terminal domain. USP35 has full enzymatic activity only when it is in its dimeric state containing the insertion region in its catalytic domain. The structural analysis reveals that USP35 without the C-terminal domain in solution exists in monomeric form, as found in the crystal structure reported earlier [2], and the monomeric form without the C-terminal domain degrades faster than USP35 with the C-terminal domain. CHIP binds and ubiquitinates USP35 by interacting with HSP90. However, CHIP-induced ubiquitination of USP35 exhibiting full activity has not been observed. That is, USP35 reverses its own ubiquitination through its own DUB activity. These structural characteristics and activity regulation ultimately affect USP35 function, which is essential for the deubiquitination of Aurora B and the control of mitosis.

Materials and methods

Plasmids and siRNAs

A p3XFlag-CMVTM7.1-hUSP35 was purchased from GenScript. The catalytic inactive USP35 mutant (USP35^{C450A}) was generated by PCR-based site-directed mutagenesis using p3XFlag-CMVTM7.1-hUSP35 as a template. All Flag-USP35 constructs were generated by PCR-base cloning using p3XFlag-CMVTM7.1-hUSP35 as a template. Myc-CHIP WT, Myc-CHIP^{K50A}, and Myc-CHIP^{H260Q} clones were kinds of gifts from Prof. Jaewhan Song (Yonsei Univ.), and Myc-Aurora B and HA-Aurora B clones were provided from Prof. Chang-Woo Lee (Sungkyunkwan Univ.). Ubiquitin and other DNAs were cloned into pCS2-His, or -HA vectors for expression in mammalian cells. Control siRNA and siRNA targeting USP35, HSP90 or CHIP were synthesized from Bioneer. siRNA sequences are as follows: HSP90, 5'-AAG CACAACGATGATGAACAG-3'; CHIP, 5'-CCAGCTGGA GATGGAGAGCTA-3', USP35, 5'-GGGAAGATCTGATGA TGTT-3'.

Cell culture and transfection

HEK293T cells and HeLa cells purchased from Korea Cell Line Bank (KCLB) were cultured in Dulbecco's modified Eagle medium (DMEM) containing 10% fetal bovine serum

and 1% penicillin and streptomycin and maintained at 37 °C in 5% CO₂. All the cell lines used in this study have been authenticated by KCLB and confirmed to be free of mycoplasma contamination prior to use. For transient transfection, HEK293T cells were transfected with plasmids using 2 M CaCl₂ and 2× HBS buffer (50 mM HEPES, 10 mM KCl, 12 mM Glucose, 280 mM NaCl, 1.5 mM Na₂HPO₄, pH 7.05) and HeLa cells were transfected with plasmids or siRNAs using Lipofectamine™ 2000 (Invitrogen) following the manufacturer's instructions. For HSP90 inhibition, Geldanamycin (GA, Santa Cruz) or PU H71 (PU, TOCRIS) was treated as indicated concentration for 24 h in the cells. MG132 (AG Scientific) and Cycloheximide (Sigma-Aldrich) were used indicated concentration and time in legends.

Western blot analysis

Western blot analyses on 10–50 µg protein extract from HEK293T cells or HeLa cells. Briefly, we lysed the cells using protein lysis buffer (50 mM Tris–Cl, 150 mM NaCl, 1% Triton X-100, 1 mM EDTA, 200 mM Na₃VO₄, 1X protease inhibitor, pH 7.4) and measured the protein concentration using Micro BCA™ Protein Assay kit (Thermo Scientific) based on the standard curve using BSA. The following antibodies were used for immunoblot analysis; rabbit anti-USP35 (A302-290A, dilution ratio 1:1000) and rabbit anti-Aurora B (A300-431A, 1:1000) were purchased from Bethyl Laboratories. Mouse anti-c-Myc (sc-40, 1:1000), was provided by Santa Cruz Biotechnology. Mouse anti-Flag (F1804, 1:1000) and Rabbit anti-HA (H6908, 1:1000) were purchased from Sigma Aldrich. Rabbit anti-Ubiquitin (#3933, 1:2000), rabbit anti-AKT (#9272, 1:1000) and rabbit anti-CHIP (#2080, 1:1000) were purchased from Cell signaling. Mouse anti-HSP90α/β (sc-13119, Santa Cruz Biotechnology, 1:5000), rabbit anti-α-tubulin (sc-Santa Cruz Biotechnology, 1:1000), and rabbit anti-β-actin (LF-PA0207, AbFrontier, 1:5000) were used to assess equal loading. Samples were analyzed by sodium dodecyl sulfate–polyacrylamide gel electrophoresis (SDS-PAGE) and western blot and chemiluminescence was measured using the Ez-Capture MG imaging system (ATTO Corporation).

Immunoprecipitation

HEK293T cells transfected with various plasmids as indicated for 24 h were collected and lysed using protein lysis buffer. About 3 mg of lysates were incubated with Flag-magnetic beads (Sigma Aldrich) for 4 h at 4 °C. Immunocomplexes were washed with lysis buffer and eluted and

boiled in 6× SDS sample buffer. For fully endogenous immunoprecipitation, about 5 mg of lysates from HEK293T cells were incubated with mouse IgG (sc-2027, Santa Cruz Biotechnology, 1 µg/1 mg lysates) or mouse anti-HSP90α/β (sc-13119, Santa Cruz Biotechnology, 1 µg/1 mg lysates) for 12 h at 4 °C. After incubation, protein G agarose beads (Thermo Scientific) were added and incubated again for 4 h at 4 °C. Immunocomplexes were washed with lysis buffer and eluted and boiled in 6× SDS sample buffer. All samples were detected by western blot analysis using the indicated antibodies, and 5% of the samples were used to identify immunoprecipitation efficiency.

Ni-NTA-mediated pulldown assay

HEK293T cells were transfected with His-ubiquitin and tagged plasmids as indicated and then treated with 10 µM MG132 (A.G. Scientific. Inc.) for 4 h. The cells were lysed with Urea lysis buffer (8 M Urea, 0.3 M NaCl, 50 mM Na₂HPO₄, 50 mM Tris–HCl, 1 mM phenylmethylsulfonyl fluoride (PMSF), 10 mM Imidazole, pH 8) and sonicated. About 3–5 mg of lysates were incubated with Ni-NTA agarose (Qiagen) for 6 h at 4 °C. The beads were washed with Urea washing buffer (8 M Urea, 0.3 M NaCl, 50 mM Na₂HPO₄, 50 mM Tris–HCl, 1 mM PMSF, 20 mM Imidazole, pH 8) and eluted in 6× SDS sample buffer. The samples were detected by western blot analysis.

Immunofluorescence

HeLa cells transfected with USP35-targeting siRNA alone or in combination with Flag-USP35 constructs were grown on glass coverslips. The cells were fixed with cold methanol for 15 min on ice and permeabilized with 1× PBS containing 0.25% Triton X-100. After washing, the cells were incubated with rabbit anti-TPX2 (1:1000) for 2 h at RT, followed by Alexa fluor-488-conjugated goat anti-rabbit IgG (Molecular Probes, 1:300) for 1 h at RT. DNA was detected with DAPI (Sigma Aldrich). The cells were visualized using 100× magnification on an LSM700 Confocal Laser Scanning Microscopy (Carl-Zeiss) and analyzed using ZEN 2012 imaging software (Carl-Zeiss).

Deubiquitinating enzyme activity assay

In vivo DUB activity of USP35 was tested using 100 ng of recombinant K48- and K63-linked polyubiquitin chains (Boston Biochem) or 100 ng of recombinant K11-, K48-, and K63-linked tetra ubiquitins. HEK293T cells transfected with p3XFlag-CMVTM7.1 vector or indicated constructs of

p3XFlag-USP35 were collected and lysed using protein lysis buffer. About 3 mg of lysates were incubated with Flag-magnetic beads for 4 h at 4 °C. The beads were washed with lysis buffer and eluted in DUB buffer (20 mM HEPES at pH 7.4, 100 mM NaCl) with 3XFlag peptide (Sigma Aldrich) for 30 min at 4 °C. The eluted samples and 100 ng recombinant ubiquitin chains were mixed with 5 mM dithiothreitol (DTT) and reacted for 15 min at 30 °C. These reactions were stopped by adding 6× SDS sample buffer. The samples were detected by western blot analysis using an anti-ubiquitin antibody. In vitro DUB activity was measured at room temperature using the cleavage-sensitive fluorogenic substrate Ub-AMC (Boston Biochem, U-550). All measurements were performed in non-binding 384-well plates with a reaction volume of 100 µl. Fluorescence intensities were measured at a wavelength of excitation wavelength of 355 nm and an emission wavelength of 426 nm using the Spectramax M3 microplate reader (Moleculardevices). The initial substrate stock solution was prepared according to the manufacturer's instructions and diluted to a concentration of 5 µM in assay buffer (20 mM HEPES pH 7.5, 150 mM NaCl, 1 mM DTT). The enzymes were diluted to a concentration of 6 µM using the assay buffer. The plate was prepared with 50 µl assay buffer, to which a 20 µl substrate solution was added. The reaction was started upon the addition of 30 µl enzyme solution. Measurements were taken every minute for 90 min and then every 1.5 min. Curves measured in triplicate were fitted using nonlinear regression analysis in Originpro 9.0 software.

Quantitative RT-PCR analysis

Total RNA from cells was extracted using RNeasy Mini Kit (Qiagen). cDNAs were synthesized using ReverTra Ace® qPCR RT Master Mix (Toyobo) and analyzed using SYBR® Green Realtime PCR Master Mix (Toyobo) on a CFX Connect™ Real-Time PCR (Bio-Rad). Primers were designed using OligoPerfect™ Designer (Invitrogen). All data were normalized to *GAPDH* expression. Primer sequences are as follows: *USP35*-F, TCGAATCTGTCAGCAACGTC; *USP35*-R, TGTCTTTGGAAATGGCTTCC; *CHIP*-F, TCAAGGAGCAGGGCAATCGTCT; *CHIP*-R, GCATCTCAGGTAGCACAAGGC; *HSP90*-F, TCTGCCTCTGGTGATGAGATGG; *HSP90*-R, CGTTCACAAAGGCTGAGTTAGC; *GAPDH*-F, CAAGATCATCAGCAATGCCTCC; *GAPDH*-R, GGTCATGAGTCCCTCCACGA.

Expression and protein purification

Constructs comprising residues USP35eCDC (aa 390–1018) and USP35eCDΔi (aa 390–926Δ603–760) of human USP35 (Swiss Prot entry: Q9P2H5) were subcloned into pCDNA3.1Myc-His vector (Invitrogen), and

produced using the FreeStyle™ 293 Expression system (Invitrogen). Briefly, FreeStyle™ 293-F cells were simultaneously transfected with expression vectors for 390–1018 and 390–926(Δ603–760) of human USP35 using 293fectin (Invitrogen), and grown in serum-free FreeStyle™ 293 Expression medium (Invitrogen) for 72 h. The conditioned media were clarified by centrifugation and passed through HiTrap™ Q HP anion exchange column (GE Healthcare) and eluted with a linear gradient of 1 M NaCl in 20 mM HEPES (pH 7.4) 1 mM TCEP. The elution proteins after centrifugation were applied to a nickel-chelated Hi-Trap column (GE Healthcare) and eluted with a linear gradient of 25–500 mM imidazole in 20 mM HEPES (pH 7.4) and 150 mM NaCl, 1 mM TCEP. For the final step, size-exclusion chromatography on HiLoad 26/60 Superdex-200 column (GE Healthcare) pre-equilibrated with 20 mM HEPES (pH 7.4), 150 mM NaCl, 1 mM DTT was carried out.

For the Ub-AMC assay and structural studies four constructs, USP35eCDC (aa 390–1018), USP35eCDΔi (aa 390–1018Δ603–760), USP35eCD (aa 390–978), and USP35eCDΔi (aa 390–978Δ603–760), of USP35 were cloned into the pGEX4T-1 vectors (Novagen). Expression was carried out in *E. coli* Rosetta2(DE3) cells (Merck) that were chemically transformed with an expression vector and subsequently grown in an LB medium supplemented with ampicillin (100 µg/ml). Cultures were grown at 37 °C for 3–4 h until an OD600 of 0.6 and then cooled to 18 °C for 1 h. Expression was induced by the addition of 0.5 mM isopropyl-β-D-1-thiogalactopyranoside (IPTG) and cultures were kept shaking at 18 °C for o/n. The cells were harvested by centrifugation and the pellet was re-suspended in buffer containing 20 mM HEPES (pH 7.4), 200 mM NaCl and 5 mM β-mercaptoethanol and then subsequently disrupted by sonication. The crude lysate was centrifuged at 18,000 rpm for 1 h at 4 °C and the cell debris was discarded. The supernatant was applied to a GStap™ FF (GE Healthcare) and eluted with 25 mM glutathione (GSH) in 20 mM HEPES (pH 7.4), 200 mM NaCl and 5 mM β-mercaptoethanol followed by digestion with thrombin (1:5 molar ratio) for o/n. It was further purified by gel filtration chromatography on HiLoad 26/600 Superdex-200 column (GE Healthcare) pre-equilibrated with the buffer consisting of 25 mM HEPES (pH 7.4) and 200 mM NaCl.

Asymmetrical flow field-flow fractionation with multi-angle light scattering (AF4-MALS) analysis

The molecular weight of USP35eCDΔi (aa 390–926Δ603–760) and USP35eCDC (aa 390–1018) were determined using the AF4-MALS detector system (Wyatt

Technology) equipped with a standard channel (25 cm), 350- μ m spacer, and regenerated cellulose membrane (10 kDa cutoff). DAWN Heleos II 18-angle MALS system with Optilab T-rEX refractive index detector was used, and data were analyzed using the Zimm model for fitting experimental light scattering data and graphed using an EASI graph with a UV peak in ASTRA 6.1 software (Wyatt Technology). About 150 μ g of USP35eCD Δ i and USP35eCD were injected in each run. The WTC-030S5 column (Wyatt Technology) was run with buffer containing 20 mM HEPES (pH 7.4), 150 mM NaCl, and 1 mM DTT at a flow rate of 0.7 ml/min at 25 °C. The ASTRA 6.1 software was used to calculate the molecular mass using BSA as a control protein.

Small-angle X-ray scattering (SAXS) data collection and analysis

The SAXS data were collected in ten successive frames per second at a flow rate of 0.3 μ l/s through a Microlab 600 advanced syringe pump (Hamilton). There was no radiation damage detected during the scattering measurements. Measurements of protein solutions were carried out over a small concentration range of 0.8–2.0 mg/ml, to obtain good-quality scattering data without any interferences of protein molecules. Data were normalized to the intensity of the transmitted beam and radially averaged. The scattering of 20 mM HEPES (pH 8.4) buffer solution was used as the experimental background. The SAXS data of USP35eCD Δ i, USP35^{C405S}eCD Δ i, and USP35eCDC fit well with the theoretically calculated model based on the Guinier plot. For USP35eCD Δ i, the radius of gyration (R_g) and maximum interatomic distance (D_{max}) values were calculated to be 24.6 ± 0.2 and 80.0 Å, respectively. The corresponding values were 49.6 ± 0.2 and 171.8 Å for USP35^{C405S}eCDC and 65.4 ± 2.5 and 232.0 Å for USP35eCDC. The molecular mass derived from the estimated Porod volume was almost similar to the calculated (see Table 1). To reconstruct the

molecular shapes, the ab initio shape determination program GASBOR [22] was used. For comparison of the overall shape and dimension, the ribbon presentation of the atomic crystal models (PDB: 5TXK) is superimposed onto the reconstructed dummy residues models using the program SUPCOMB [23].

Statistical analysis

Results are shown as mean \pm SD of at least three independent experiments unless otherwise indicated in the Fig. legends. The comparison of different groups was carried out using a two-tailed unpaired Student's *t* test, and the *P* value < 0.05 was considered statistically significant and reported as in legends.

Results

The C-terminal domain and the insertion region in the USP domain are required for full USP35 activity

Amino acid (aa) sequence alignment showed that the sequence from the USP domain (catalytic domain, CD: aa 440–926) to the C-terminal domain (CTD, aa 926–1018) of USP35 are highly conserved among the species, while the insertion region (i, aa 603–760) within the USP domain varies, even among vertebrates (Supplementary Fig. 1). To gain insights into the insertion region and the C-terminal domain of human USP35, we designed various constructs with boundaries based on previously reported studies and secondary structure predictions [2] (Fig. 1a). First, we examined the DUB activity of USP35 variants by performing experiments using immunoprecipitated USP35 in cell lysate. USP35CD did not cleave the K48-linked polyubiquitin

Table 1 Structural parameters obtained from the SAXS data of truncated and full-length proteins in solution

Sample	$R_{g,G}^a$ (Å)	$R_{g,p(r)}^b$ (Å)	D_{max}^c (Å)	$MM_{calculated}^d$ (kDa)	MM_{SAXS}^e (kDa)
USP35 390–926 Δ 605–760	24.25 ± 0.24	24.62 ± 0.19	80.0	45.0	43.4
USP35 440–1018 Δ 605–760:Ubiquitin	48.04 ± 1.54	49.63 ± 0.17	171.8	55.8	113.7
USP35 390–1018	67.66 ± 3.32	65.37 ± 2.50	232.0	140.0	166.1

^a $R_{g,G}$ (radius of gyration) was obtained from the scattering data by the Guinier analysis

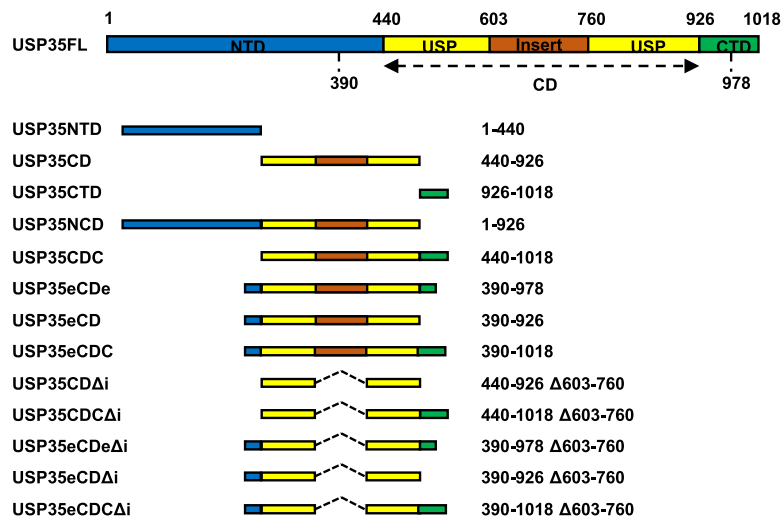
^b $R_{g,p(r)}$ (radius of gyration) was obtained from the $p(r)$ function by the program GNOM

^c D_{max} (maximum dimension) was obtained from the $p(r)$ function by the program GNOM

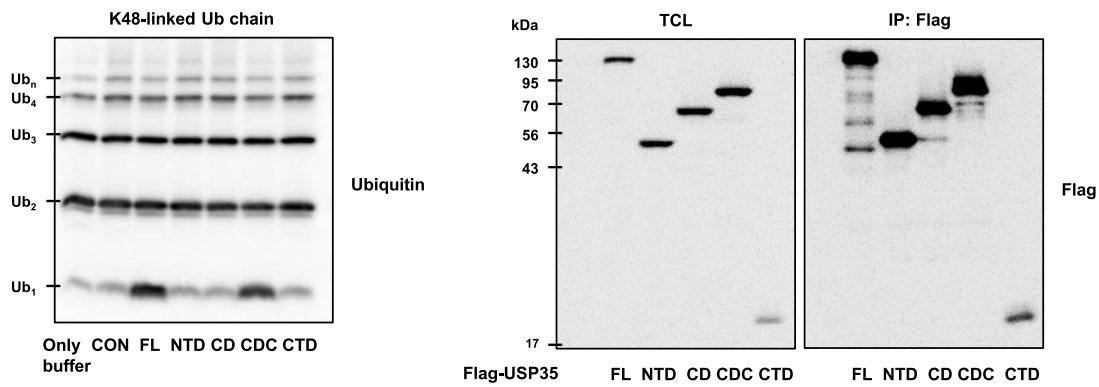
^d $MM_{calculated}$ (molecular mass) was obtained from the amino acid sequence of the protein

^e MM_{SAXS} (molecular mass) was estimated from a BSA standard protein

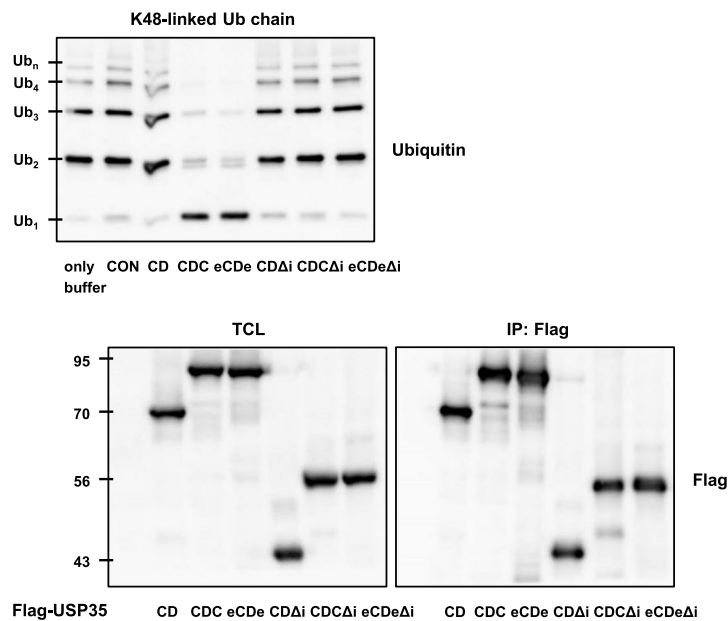
a



b



c



d

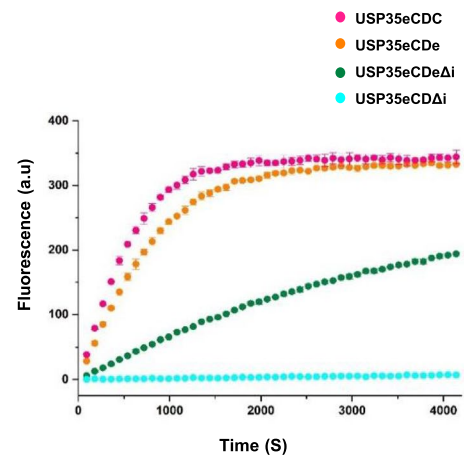


Fig. 1 The insertion region and C-terminal domain are required for full USP35 activity. **a** USP35 constructs used in experiments. **b, c** HEK293T cells were transfected with the indicated Flag-USP35 constructs. The cell lysates were incubated with K48-linked polyubiquitin chains for 15 min after immunoprecipitation with an anti-Flag antibody. Cleaved ubiquitin chains were detected by immunoblotting with an anti-ubiquitin antibody. **d** In vitro DUB activity using Ub-AMCs

chain although the USP domain is a catalytic domain that includes the active cysteine residue C450. However, USP35 with both the USP and C-terminal domains (USP35CDC, aa 440–1018), cleaved the aforementioned ubiquitin chains, similarly to that of full-length USP35 (FL, aa 1–1018). Neither the N-terminal domain (NTD, aa 1–440) nor the C-terminal domain alone showed activity (Fig. 1b). The same outcomes were observed in analyses of K63-linked polyubiquitin chains (Supplementary Fig. 2). Therefore, we concluded that the C-terminal domain and the catalytic domain of USP35 are critical to its DUB activity.

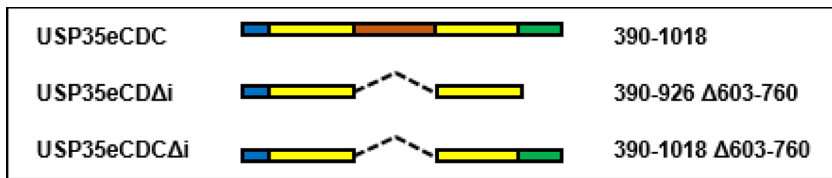
Previously, Kurathu and colleagues reported that either the extended USP domain (eCDe, aa 390–978) or the extended USP domain with the insertion deleted (eCDe Δ i, aa 390–978 Δ 603–760) in USP35 showed enzymatic activity in an in vitro DUB assay [2]. Since the only USP domain in USP35 did not show activity in vivo, we cloned the same fragments as those described in the paper and verified their DUB activity. When several USP35 constructs were transfected in HEK293T cells and immunoprecipitation was performed with an anti-Flag antibody, the results showed that USP35eCDe cleaved K48-linked polyubiquitin chains, but USP35CD did not cleave these chains (Fig. 1c). Considering this result, we provided evidence that residues 926–978 in the C-terminal domain are important for the activity of USP35. However, we did not see any disassembly of these chains in the insertion-deleted mutants of USP35, such as USP35CD Δ i (aa 440–926 Δ 603–760), USP35eCDe Δ i (aa 390–978 Δ 603–760), or USP35eCDC Δ i (aa 390–1018 Δ 603–760) in vivo (Fig. 1c). We proposed two possibilities to explain the reasons that our results differ from previous results. First, we used a small concentration of K48-linked polyubiquitin chains (100 ng) and HEK293T cell lysates for the in vivo DUB assay. Second, the reaction time in which the ubiquitin chains were cleaved was shorter (15 min) than that in previously performed in vitro experiments. To more clearly confirm the role of the insertion region, we characterized the DUB activity of recombinant USP35 constructs using a minimal synthetic substrate, ubiquitin fused to a C-terminal fluorescent group (Ub-AMC), in a hydrolysis assay. Since the expression levels of the USP35 constructs

in which residue 440 was the first aa in *E. coli* were low, we produced four USP35 constructs with residue 390 as the first aa (USP35eCD Δ i, USP35eCDe Δ i, USP35eCDe, and USP35eCDC). Consistent with the in vivo DUB activity, USP35 with the USP domain and C-terminal domain, at least, residues 926–978 (USP35 eCDe and USP35eCDC) showed very similar activity, but the USP domain without the insertion region (USP35eCD Δ i, aa 390–926 Δ 603–760) showed considerably less activity. Interestingly, the USP35 construct with the C-terminal domain without the insertion region in the USP domain (USP35eCDe Δ i) showed approximately one-half the catalytic activity as that of the USP35 eCDe construct (Fig. 1d). On the basis of these data, we demonstrated that USP35 showed full DUB activity when both the insertion region and C-terminal domain comprising at least residues 926–978, were included in the fragment.

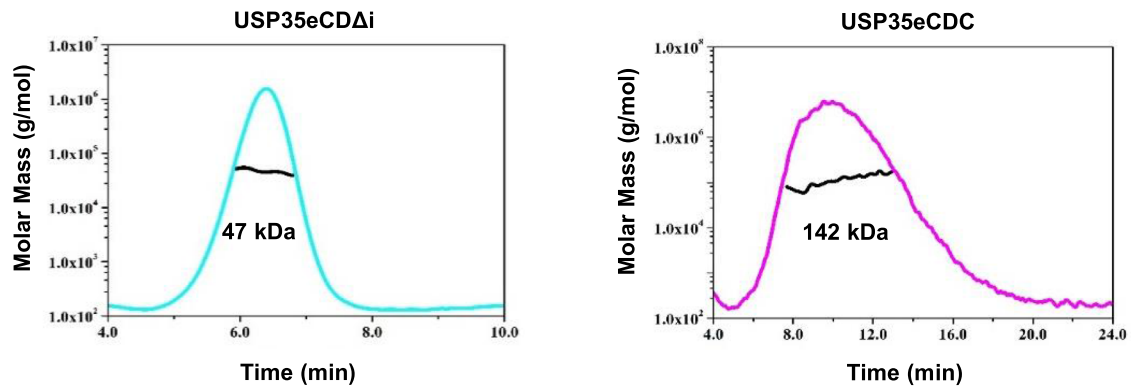
Recombinant USP35 that includes the C-terminal domain forms dimers

To understand how the insertion region and C-terminal domain affect the DUB activity of human USP35, we attempted to address this based on the structural point of view. Recombinant USP35 sequences with residue 390 as the first aa, such as USP35eCDC and USP35eCD Δ i, were purified from FreeStyle™ 293-F cells. Through asymmetrical flow field-flow fractionation with multiangle light scattering (AF4-MALS), the oligomeric state of these proteins in solution was analyzed. While USP35eCD Δ i was eluted as a monomer (47.6 kDa), USP35eCDC behaved as a dimer with a Mr of 142.7 kDa (Fig. 2a). This finding suggested that the C-terminal domain and/or the insertion region is involved in dimer formation.

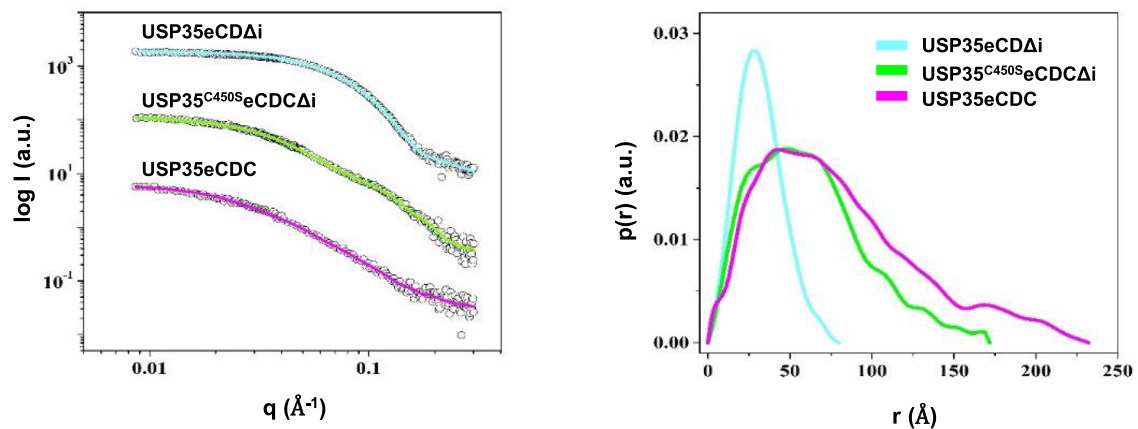
To further assess the possible orientation of the insertion region and conformation of the C-terminal domain, we attempted both crystallization and small-angle X-ray scattering (SAXS), which can provide information on the shape of molecules in solution [24]. Three recombinant proteins containing the USP domain and the C-terminal domain with or without the insertion region, namely USP35eCDC, USP35eCDC Δ i, and USP35eCD Δ i in *E. coli*, were used. To establish USP35eCDC Δ i, we generated the catalytically inactive mutant USP35^{C450S}, and ubiquitin was co-expressed for stability. Although we failed to obtain diffraction-quality crystals, we were able to collect SAXS data. The initial fit of the SAXS data on the USP35 proteins included Guinier and pair distance distribution fit with respect to the radius of gyration (Rg) and maximum distance (Dmax), respectively (Fig. 2b and Table 1). An analysis of the scattering



a



b



c

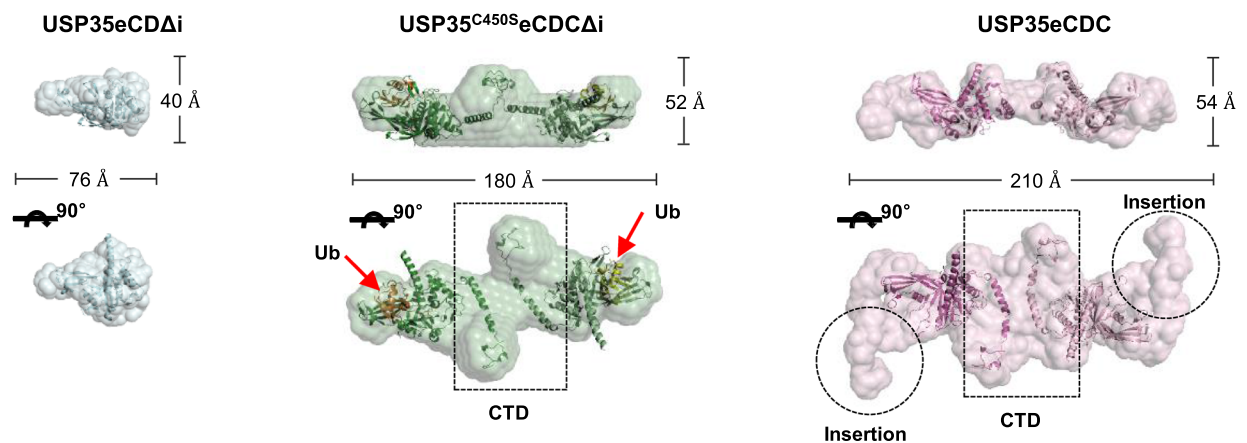


Fig. 2 Recombinants USP35 containing the C-terminal domain form a dimer. **a** AF4-MALS for USP35CD Δ i (left) and USP35eCDC (right) proteins in solution. The thick black lines represent the molecular weight as determined by the Zimm model. **b** $I(q)$ versus q in log–log plots of USP35eCD Δ i (blue line), USP35eCDC Δ i (green line) and USP35eCDC (red line) protein in solution. Open shapes represent the experimental data, and solid lines represent the X-ray scattering profiles obtained from dummy residue models using GASBOR. For clarity, each plot is shifted along the log $I(q)$ axis (left). The pair distance distribution $p(r)$ functions of the USP35eCD Δ i (blue), USP35eCDC Δ i (green) and USP35eCDC (red) proteins in aqueous solution were based on an analysis of the experimental SAXS data using the program GNOM. The areas under the curves were normalized to molecular weight for ease of comparison (right). **c** Structural envelopes of USP35eCD Δ i, USP35eCDC Δ i, and USP35eCDC were obtained using the ab initio shape method program GASBOR with P2 symmetry restriction. Surface rendering was achieved using the PyMOL program. The ribbon presentation of the crystal structure of USP35 with bound Ub (PDB: 5TXK), and the predicted α -helix in the C-terminal domain (generated using PYRE2.0) is superimposed onto the constructed envelope using the program SUPCOMB. Ubiquitin is orange. The possible positions of the C-terminal domain and the insertion region are indicated

data indicated that the catalytic domain with both the insertion region and C-terminal domain deleted (USP35eCD Δ i) was a monomer with a molecular mass of ~43 kDa and an estimated D_{\max} of ~80 Å (Fig. 2c). These results were nearly the same as those obtained with the crystal structure of the ubiquitin-bound catalytic domain of USP35 [2] (PDB: 5TXK). However, USP35^{C450S}eCDC Δ i and USP35eCDC showed molecular masses of ~114 and 166 kDa, respectively, which were significantly larger than the mass of USP35eCD Δ i. The $P(r)$ data of USP35eCDC Δ i^{C450S} and USP35eCDC revealed similar profiles, with D_{\max} values of ~171 Å and 232 Å, respectively. Therefore, these mutants formed homodimers, and the C-terminal domain was associated with the dimeric state. The D_{\max} for USP35eCDC was considerably larger than that of USP35^{C450S}eCDC Δ i, which may indicate that the insertion region adopts an extended conformation with a high degree of flexibility. In conclusion, both the MALS and SAXS data indicated that the C-terminal domain plays a role in dimer formation, whereas the insertion region likely to be quite flexible (Fig. 2c).

USP35 exhibits auto-deubiquitination

USP35 exhibited full enzymatic activity when it has the insertion in the dimeric form through the C-terminal domain. However, although the stability of USP35 with full activity was maintained, USP35 in a monomeric state was rapidly degraded when CHX was added to the cells (Fig. 3a). From the results obtained thus far, we deduced that the catalytic

activity of USP35 is necessary to prevent its degradation. To determine whether the degradation of USP35 is due to ubiquitination, we transfected USP35 truncation mutants into HEK293T cells and analyzed the status of ubiquitination through a Ni–NTA pulldown assay. Only USP35CD was ubiquitinated in the presence of ubiquitin. However, we did not observe ubiquitinated forms of either USP35FL or USP35CDC, which both included the USP domain (Fig. 3b). Interestingly, USP35CD was ubiquitinated when we added the C-terminal domain (USP35CTD) in trans to the cells (Fig. 3b), suggesting that the USP domain of USP35 is ubiquitinated, but when the C-terminal domain comprises the same chain (USP35CDC), in cis, ubiquitination was suppressed. In addition, the USP domain without the insertion region (USP35CD Δ i) was ubiquitinated, demonstrating that the ubiquitination site of USP35 might be in the USP domain but not the insertion region (Fig. 3c). Indeed, the ubiquitinated form was not identified when in the USP35 construct with an extended USP domain (USP35eCDe), but when the extended USP domain lacked the insertion region (USP35eCDe Δ i), the construct was ubiquitinated (Fig. 3c). On the basis of these results, we concluded that USP35 is not ubiquitinated in the dimer state when both the insertion region within the USP domain and at least residues 926–978 were included.

To explain the reason that USP35 with full activity is not ubiquitinated, we hypothesized that USP35 with enzymatic activity continually cleaves ubiquitin chains from itself. To determine whether USP35 can remove the ubiquitin chains attached to its own USP domain, we co-transfected HEK293T cells with His-Ubiquitin, HA-USP35CDC^{C450A}, and several Flag-USP35 constructs and performed an ubiquitination assay with Ni–NTA agarose. The ubiquitination of HA-USP35CDC^{C450A} was decreased by the overexpression of Flag-USP35FL, Flag-USP35CDC, or Flag-USP35eCDe. Thus, USP35 with full enzymatic activity disassembled the ubiquitin chains attached to the catalytically inactive form of USP35 (USP35CDC^{C450A}). In addition, USP35CD Δ i and USP35eCDe Δ i did not affect the ubiquitination of USP35 inactive form, suggesting that USP35 with an intact insertion region in the USP domain and the C-terminal domain (at least aa 926–978) showed auto-deubiquitination activity (Fig. 3d). To further investigate whether the N-terminal domain is involved in the activity of USP35, we designed a USP35 construct containing the USP domain and N-terminal domain (USP35NCD, aa 1–926) (Fig. 1a) and tested its ubiquitination and catalytic activity. In contrast to constructs with the C-terminal domain, a USP35NCD construct was

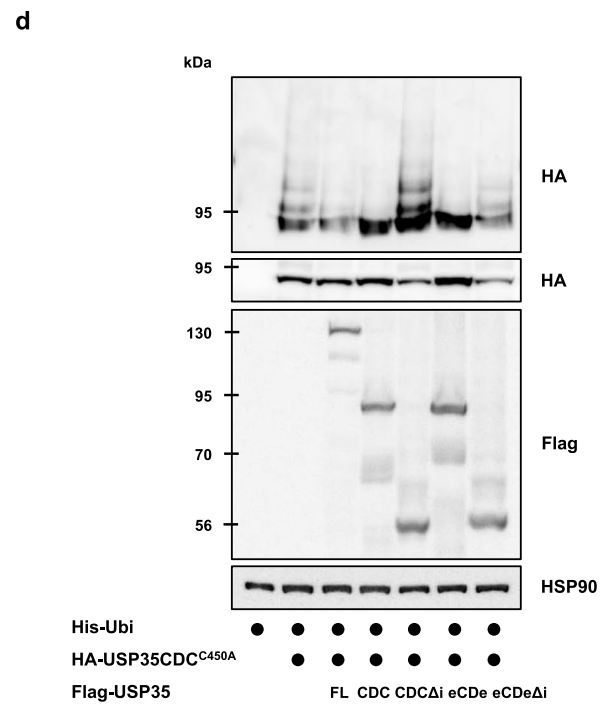
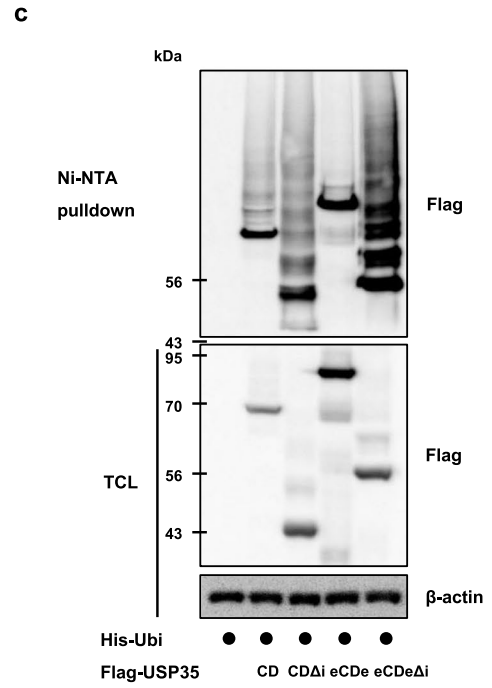
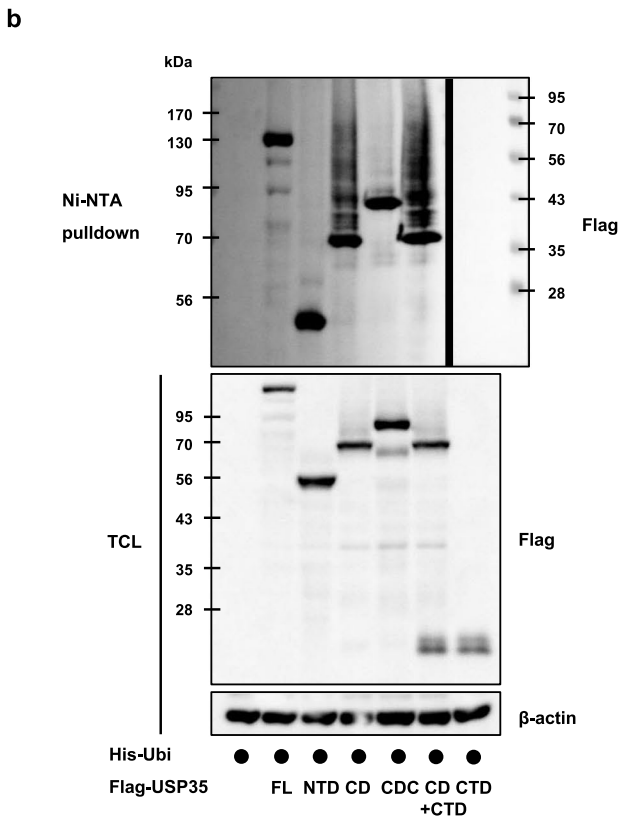
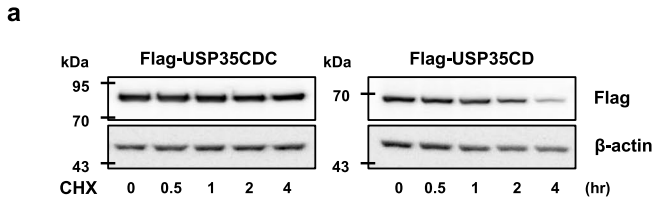
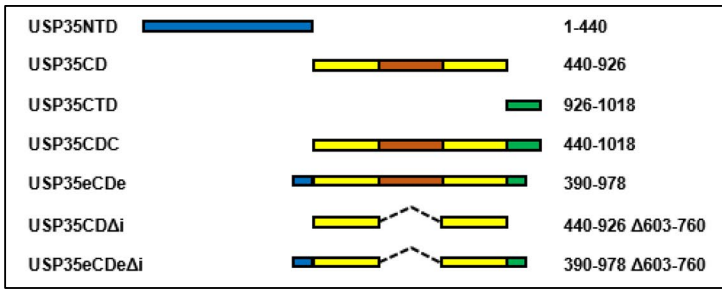


Fig. 3 Fully active USP35 functions through auto-deubiquitination. **a** HeLa cells were transfected with Flag-USP35CDC or Flag-USP35CD. The cells were then treated with 100 µg/ml cycloheximide (CHX) and harvested at the times indicated. A western blot analysis was performed to detect USP35 protein levels. **b, c** HEK293T cells transfected with His-ubiquitin alone or together with the indicated Flag-USP35 constructs were treated with MG132 for 4 h. Ubiquitination of each Flag-USP35 construct was observed using a Ni-NTA-mediated pull-down assay. **d** HEK293T cells transfected with His-ubiquitin alone or together with HA-USP35CDC^{C450A} and the indicated Flag-USP35 constructs were treated with MG132 for 4 h. HA-USP35CDC^{C450A} ubiquitination was observed by a Ni-NTA-mediated pull-down assay

ubiquitinated in the presence of ubiquitin and exhibited no DUB activity (Supplementary Fig. 3a, b).

HSP90 interacts with USP35

To find an E3 ligase that ubiquitinates USP35, we subjected HEK293T cells transfected with Flag-USP35FL to immunoprecipitation assays and LC-MS analysis (Fig. 4a). Of the several proteins pulled down, we noticed HSP90 was a partner protein of USP35. HSP90 is a typical chaperone and regulates the function of many client proteins. HSP90 regulates the stability of client proteins by controlling their folding and degradation. To achieve the folding or degradation of client proteins, HSP90 cooperates with other co-chaperones such as HOP and CHIP. When binding to HOP kinase, HSP90 facilitates client protein folding as a chaperone and helps maintain the client protein structure. However, when interacting with CHIP, which shows ubiquitin ligase activity, HSP90 has been found to facilitate the degradation of client proteins [25, 26]. By transfecting cells with wild-type Flag-USP35 (WT USP35) or catalytic inactive Flag-USP35 form, USP35^{C450A}, and HA-HSP90, we observed the interaction of USP35 with HSP90 by co-immunoprecipitation with an anti-Flag antibody (Fig. 4b). Consistent with this result, ectopically expressed Flag-USP35 or Flag-USP35^{C450A} was associated with endogenous HSP90 (Fig. 4c). In addition, USP35 interacted with HSP90 under physiological conditions (Fig. 4d). These results indicated that USP35 interacted with HSP90 and that the DUB activity of USP35 was not required for this interaction. To identify the region of USP35 that is involved in the interaction with HSP90, we performed immunoprecipitation with generated USP35 deletion mutants. Binding tests with immobilized HA-HSP90 showed that the USP domain of USP35 was critical for the interaction of HSP90 (Supplementary Fig. 4). Next, we wondered whether HSP90 regulates the degradation of USP35. When

the expression of HSP90 was decreased by siRNA, the levels of the USP35 protein were increased compared to the levels of control siRNA (Fig. 4e). To further investigate HSP90-induced changes to the levels of USP35 protein, we treated HeLa cells that had been transfected with HSP90 siRNA alone or together with Flag-USP35 or Flag-USP35^{C450A} with cycloheximide and harvested the cells for a time-course analysis. The depletion of HSP90 prevented the degradation of endogenous USP35 and ectopically overexpressed WT USP35 and USP35^{C450A} compared to the expression level observed in control cells (Fig. 4f). Indeed, overexpression or knockdown of HSP90 did not affect USP35 mRNA levels (Supplementary Fig. 5a, b). These results indicated that HSP90 regulated USP35 protein stability. In addition, an increase in USP35 protein levels induced by HSP90 knockdown enhanced USP35 catalyzed ubiquitin chains cleavage (Fig. 4g). To confirm that HSP90 activity is required for the regulation of USP35 levels, we treated cells with HSP90 inhibitors such as geldanamycin (GA) and PU-H71 (PU). However, HSP90 inhibitors exerted no effect on the level or ubiquitination status of USP35 (Supplementary Fig. 6a–c). Hence, these results showed that HSP90 regulated USP35 protein levels regardless of HSP90 activity.

CHIP binds to and ubiquitinates USP35 in an HSP90-dependent manner

As mentioned earlier, HSP90 modulates client protein levels via co-chaperon CHIP-dependent degradation. We investigated the interaction between CHIP and USP35 to determine the effect of CHIP on the USP35 level. Interestingly, wild-type CHIP (WT CHIP) and CHIP catalytic inactive form (CHIP^{H260Q}) interacted with USP35 but CHIP^{K30A}, which cannot bind to the chaperon protein, did not bind to USP35 (Fig. 5a). This result meant that CHIP interacted with USP35 in an HSP90-dependent manner. Next, we examined whether CHIP ubiquitinates USP35. Based on the auto-deubiquitinating activity of USP35, only USP35^{C450A}, but not WT USP35, was ubiquitinated by overexpressed WT CHIP, but not by CHIP^{H260Q} or CHIP^{K30A} (Fig. 5b). Indeed, HSP90 knockdown decreased the ubiquitination of USP35^{C450A}, but not WT USP35 (Fig. 5c). Additionally, CHIP-induced ubiquitination of USP35^{C450A} was decreased by HSP90 knockdown (Fig. 5d). On the basis of these data, we concluded that CHIP ubiquitinated USP35^{C450A} but not WT USP35, and that the ubiquitination of USP35^{C450A} by CHIP relied on HSP90 as well as the interaction between CHIP and USP35.

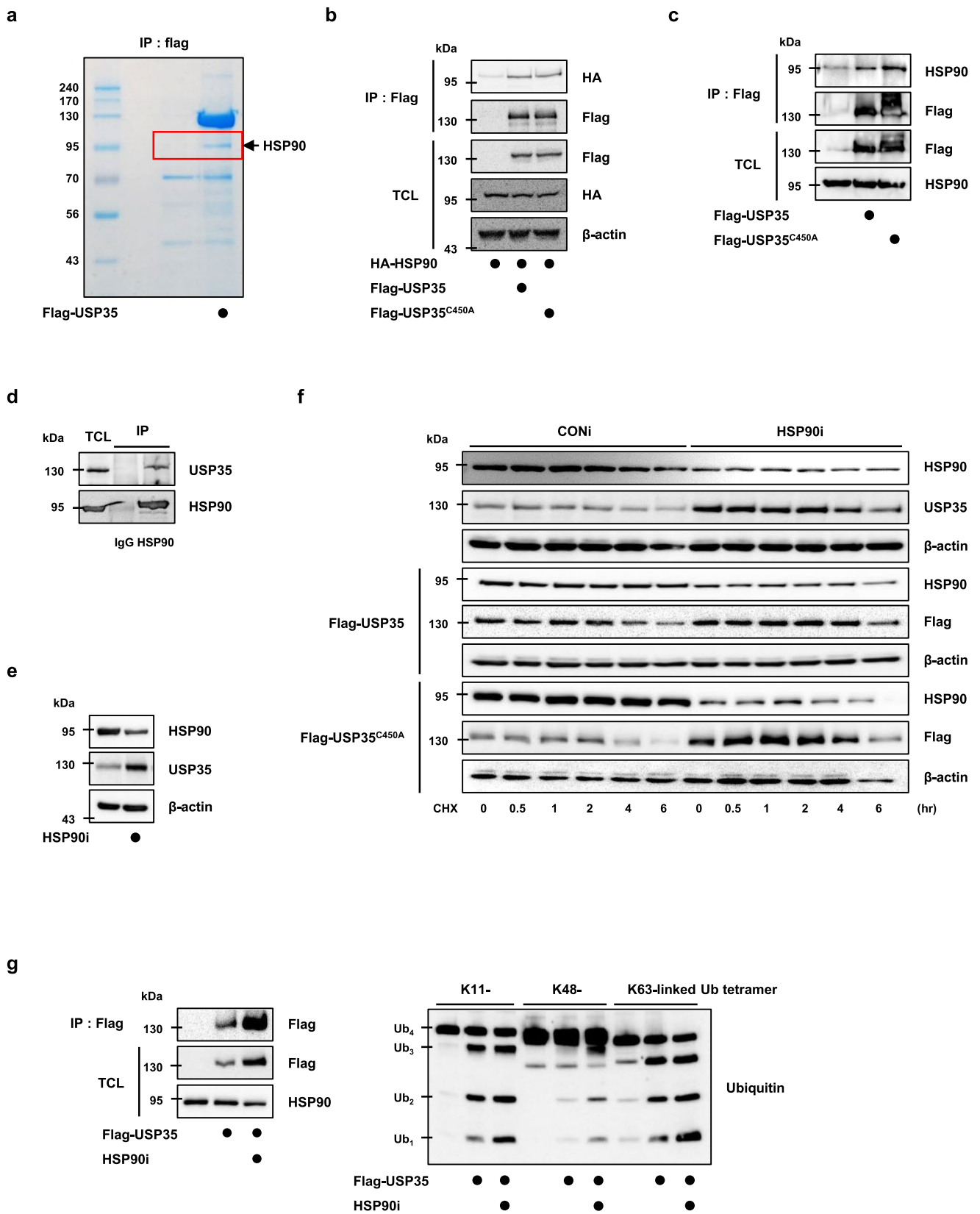


Fig. 4 HSP90 regulates the stability of USP35. **a** HEK293T cells were transfected with Flag or Flag-USP35. Cell lysates were immunoprecipitated with anti-Flag antibody, and purified proteins were separated on gels and stained with Coomassie Blue. Each specific protein band was identified by mass spectrometric analysis. **b** HEK293T cells were transfected with HA-HSP90 alone or in combination with Flag-USP35 or Flag-USP35^{C450A}. The interaction between HSP90 and USP35 was detected by immunoblotting after immunoprecipitation with an anti-Flag antibody. **c** HEK293T cells were transfected with Flag-USP35 or Flag-USP35^{C450A}. The interaction between endogenous HSP90 and Flag-USP35 was detected by immunoblotting after immunoprecipitation with an anti-Flag antibody. **d** the interaction between endogenous USP35 and HSP90 was detected by immunoblotting after immunoprecipitation with anti-HSP90 antibody. **e** HeLa cells were transfected with CONi or HSP90i. A western blot analysis was performed to detect USP35 protein levels. **f** HeLa cells were transfected with CONi or HSP90i alone or in combination with Flag-USP35 or Flag-USP35^{C450A}. The cells were then treated with 100 µg/ml CHX and harvested at the times indicated. A western blot analysis was performed to detect Flag-USP35 protein levels. **g** HeLa cells were transfected with Flag-USP35 alone or in combination with HSP90i. The cell lysates were incubated with K11-, K48 or K63-linked tetraubiquitin for 15 min after immunoprecipitation with an anti-Flag antibody. Cleaved ubiquitin was detected by immunoblotting with an anti-ubiquitin antibody

Because deficient HSP90 led to attenuated CHIP-induced ubiquitination of USP35^{C450A} and increased USP35 protein levels, we proposed that CHIP regulates USP35 protein levels. We transfected HeLa cells with USP35^{C450A} alone or together with WT CHIP and observed that the USP35^{C450A} levels were decreased by the overexpression of WT CHIP. However, when CHIP^{K30A} or CHIP^{H260Q} was overexpressed, the USP35^{C450A} level was not changed; thus, CHIP regulated USP35^{C450A} levels through ubiquitination, and this response required HSP90 (Fig. 5e). Depletion of CHIP by siRNA increased the USP35 level, as expected. (Fig. 5f). Consistent with HSP90, CHIP did not regulate USP35 expression (Supplementary Fig. 5a, b).

The USP35 dimer cleaves the ubiquitin chain attached to it by CHIP

Since we demonstrated that CHIP is an E3 ubiquitin ligase of USP35, we wanted to determine whether CHIP-induced ubiquitination is inhibited by USP35 itself. As shown in Fig. 5g, the ubiquitination of HA-USP35CDC^{C450A} was increased by CHIP, but this response was inhibited by the overexpression of Flag-USP35FL or Flag-USP35CDC. These results indicated that USP35 with full activity deubiquitinated it after CHIP had induced the ubiquitination of USP35 inactive form. All constructs of catalytic inactive USP35 mutants (USP35^{C450A}, USP35^{C450A}CD, and USP35^{C50A} CDC) were ubiquitinated by CHIP, while WT

USP35 with both the USP domain and C-terminal domain was not ubiquitinated by CHIP, suggesting that USP35 auto-deubiquitination requires active cysteine residue (Fig. 5h).

USP35 dimer regulates mitosis through deubiquitination of Aurora B

Previously, we reported that USP35 is involved in mitosis via deubiquitination of Aurora B [3]. To confirm that the activity and dimeric formation of USP35 affect cell cycle regulation, we observed the cell morphology at each phase of mitosis. When cells were transfected with siRNA targeting USP35, the number of mitotic errors was increased compared to that in the control cells, as previously reported. These defects in USP35-deficient cells were largely reversed by expression of the USP35 construct consisting of the USP domain and C-terminal domain that formed a dimer and showed full activity but not by the expression of the USP domain of USP35, which was a monomer and showed no activity (Fig. 6a). Thus, USP35 with full activity in a dimeric state is required for successful mitotic progression. USP35 targets and deubiquitinates Aurora B kinase, thus maintaining Aurora B stability during mitosis. We tested the ubiquitination of Aurora B by several USP35 deletion mutants. As expected, only fully active USP35 constructs such as USP35FL and USP35CDC deubiquitinated Aurora B (Fig. 6b).

A previous study showed that another substrate of USP35, STING bound to the C-terminal USP catalytic domain (aa 433–1018, excluding the insertion region) of USP35 [6]. To determine the domain that mediates the interaction of Aurora B with USP35, a series of USP35 truncation mutants were expressed in HEK293T cells. Our co-IP assay showed that Aurora B bound to the USP domain of USP35 (Fig. 7a). Since HSP90 is mainly bound to USP35 through the USP domain, we checked whether each protein competitively interacted with USP35 and ascertained when each protein showed greater binding. The results showed that Aurora B and HSP90 did not competitively bind USP35; that is, Aurora B or HSP90 alone or in combination showed no difference in binding to USP35 (Fig. 7b). However, the interaction between HSP90 and USP35 was weaker in mitotic cells than in normal cells, suggesting that USP35 increasingly binds to Aurora B by dissociating from HSP90, increasing the stability of Aurora B in mitosis (Fig. 7c, d).

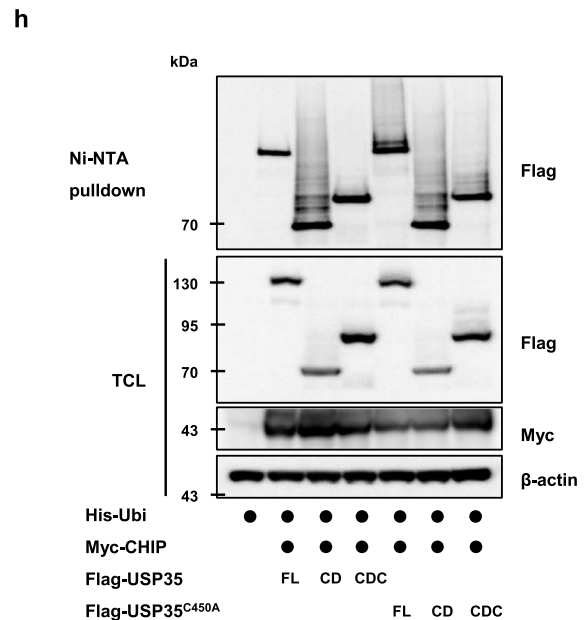
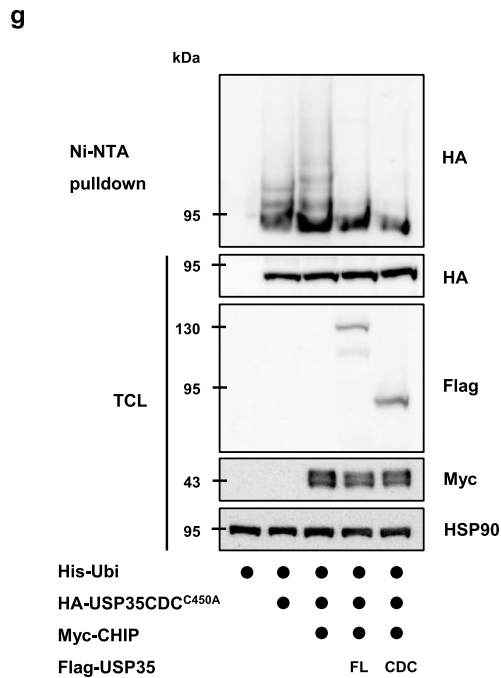
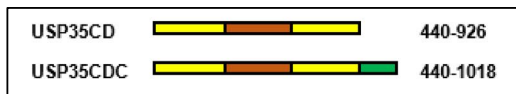


Fig. 5 (continued)

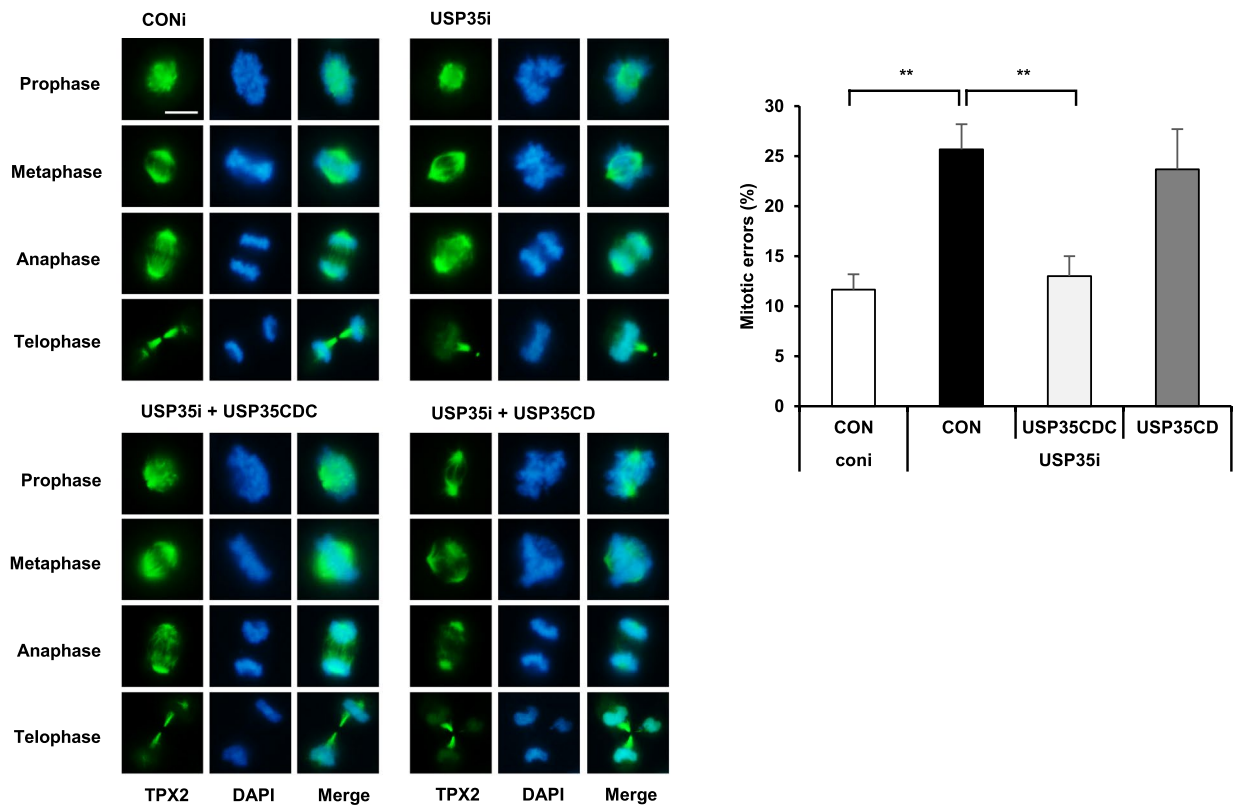
Discussion

USP35 consists of an N-terminal HEAT repeat, a USP domain with a long insertion region, and a C-terminal domain. Here, we showed that both the C-terminal domain and the insertion region within the USP domain are required for USP35 DUB activity, but that the N-terminal domain does not have any effect on its catalytic activity. Additionally, we found that the USP domain is critical for USP35 binding to other proteins and is the site where ubiquitination occurs. A HEAT repeat, a tandem repeat of a structural motif composed of two α -helices linked by a short loop, commonly forms a solenoid and mediates protein–protein interactions [27]. However, both the substrate Aurora B and the partner protein HSP90 bound to the USP domain of USP35. What role does the N-terminal domain of USP35 play? A previous study reported that the removal of residues 1- 269, which disrupts the HEAT repeat motif, enables efficient ER targeting. The authors proposed that these residues might be the binding site for proteins that

interfere with USP35 integration into the ER membrane [2]. Further studies will need to perform to find the binding protein and determine the details of its interactions with USP35.

Both the MALS and SAXS data showed that the catalytic domain and C-terminal domain of USP35 were involved in homodimer formation, although the catalytic domain without the insertion region forms a monomer both in crystalline and soluble states. In addition, both the C-terminal domain and the insertion region contribute to the full enzymatic activity of USP35. These two unexpected features from the structural studies, the presence of a distinct stable assembly of a dimer through the C-terminal domain and the implication of the long insertion in the deubiquitinating activity of USP35, are distinct from USP25 and USP28. Although USP25 and USP28 have a long insertion region of approximately 175 residues in the catalytic domain and a highly conserved C-terminal domain comprising ~350 residues, dimer formed by these proteins is achieved through the symmetric association of the insertion rods, with the

a



b

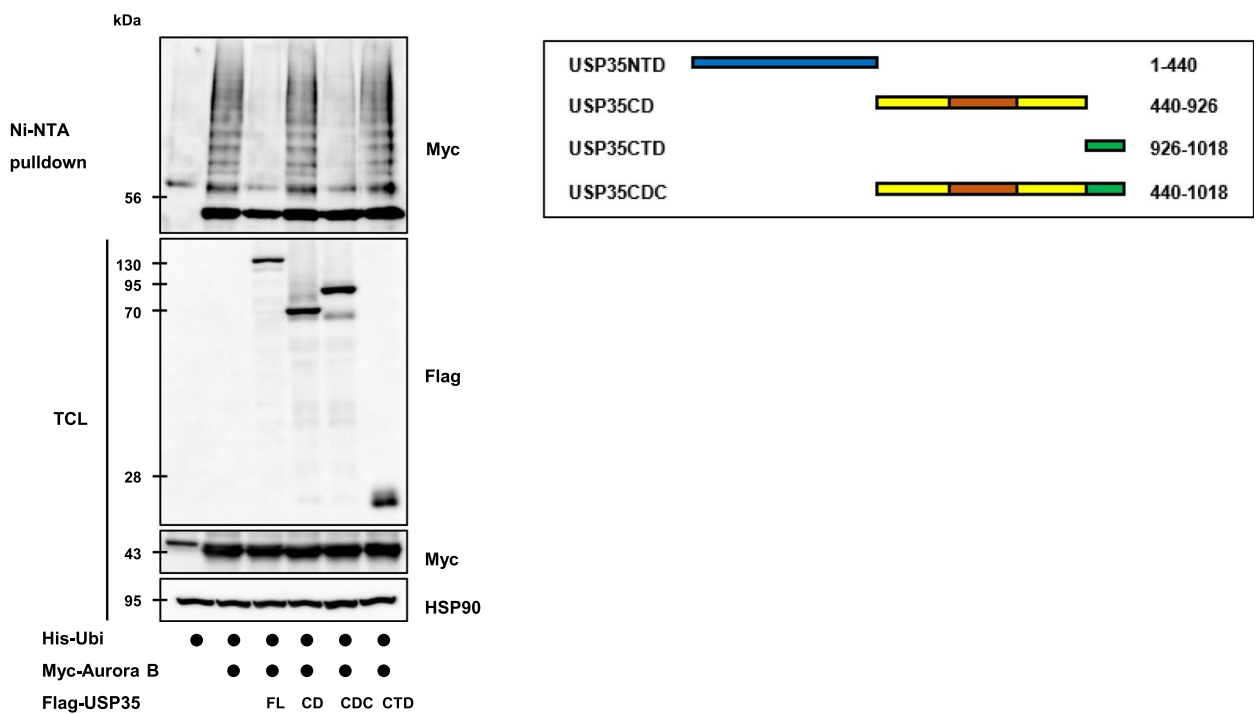


Fig. 6 A fully active USP35 dimer is required to regulate mitosis. **a** HeLa cells were transfected with USP35i alone or in combination with Flag-USP35CDC or Flag-USP35CD. Immunofluorescence staining was performed using a TPX2 antibody. One hundred cells per group were examined from three independent experiments. Scale bar 10 μm . **b** HEK293T cells transfected with His-ubiquitin alone or together with Myc-Aurora B or the indicated Flag-USP35 constructs were treated with MG132 for 4 h. Myc-Aurora B ubiquitination was observed using a Ni-NTA-mediated pull-down assay. In **a**, data are presented as mean \pm SD. $**P < 0.005$ (Student's *t* test)

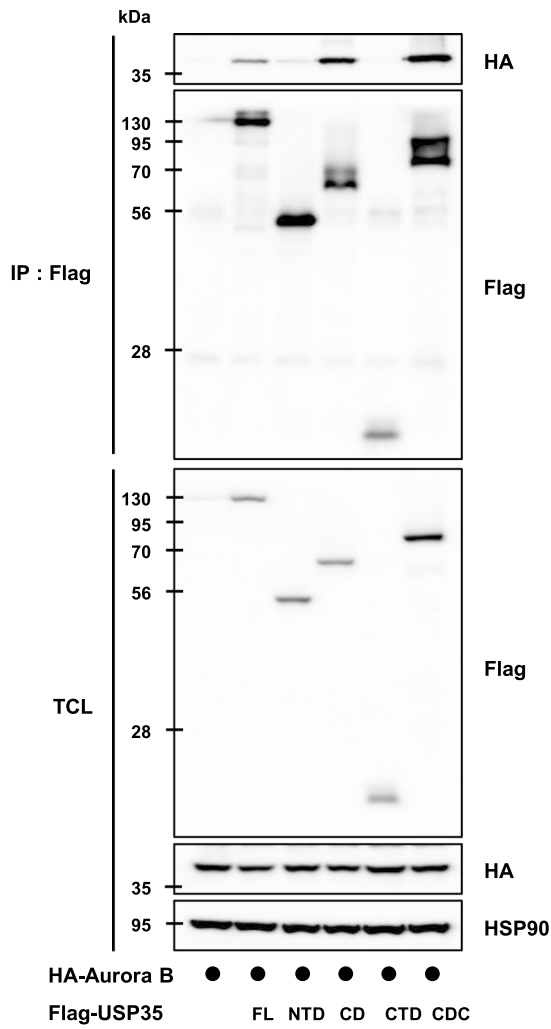
two independent catalytic sites spatially separated and the C-terminal domain exerting no impact on oligomerization. In contrast, the α -helical C-terminal domain is implicated in substrate binding in both USP25 and USP28 [13]. Moreover, USP25 dimers, but not USP28 dimers, can form auto-inhibited tetramers with the conserved insertion blocking ubiquitin binding. In the case of USP25, the crystal structure of the catalytic domain with the insertion region deleted is also a monomer [12, 13]. Although one has to wait for the crystal structure of the full-length enzyme to understand the details, it is clear that the assembly of the dimeric unit found in USP35 is unique. As stated earlier, the C-terminal domain of USP35 is highly conserved, while the insertion region shows low sequence homology (Supplementary Fig. 1). However, the insertion is near the ubiquitin-binding site. Both the C-terminal and the insertion region include several charged residues—certain stretches in the insertion consist of negatively charged residues, particularly glutamate. Secondary structure prediction programs have suggested the possible presence of two α -helices in both of these domains. Based on these findings, it is tempting to suggest that two α -helices in the C-terminal domain contribute to dimerization, but one certainly cannot rule out the possible involvement of the insertion region in the dimer formation. Additionally, we do not know the details of how the insertion region within the USP domain regulates DUB activity, but it has the potential to interfere with ubiquitin-binding since the insertion region is near the ubiquitin-binding site (Fig. 3c).

Auto-deubiquitination has been observed in a few DUBs and it has been shown to affect their functions. First, auto-deubiquitination regulates DUB localization in the nucleus and cytosolic shuttling. The monoubiquitination of several sites in the NLS region of BAP1 by UBE2O induces the cytoplasmic sequestration of BAP1 and auto-deubiquitination drives BAP1 nuclear import, where it deubiquitinates nuclear substrates. A prediction-based model suggests that intramolecular interactions between the C-terminal region and the UCH domain are required for efficient auto-deubiquitination [19]. Interactor binding can also be regulated by auto-deubiquitination. USP4 promotes homologous

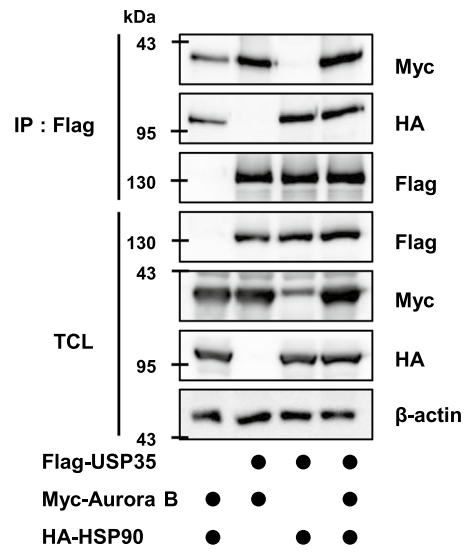
recombination-mediated DNA repair through its interaction with CtIP/MRN which is required for CtIP recruitment to DNA damage sites. The mass analysis revealed multiple ubiquitination sites in USP4, and these are deubiquitinated when USP4 shows catalytic activity. When USP4 is deubiquitinated, the interaction between CtIP/MRN and USP4 is stimulated. This means that the ubiquitination of USP4 counteracts its interactions and functions. As its most common function, a DUB with auto-deubiquitination regulates its own stability. DUBs that lose their activity, are more prone to degradation when ubiquitinated by E3 ligases [28]. USP19 removes ubiquitin via auto-deubiquitination, and a catalytically inactive mutant of USP19 is prone to degradation. USP19 is stabilized by self-association and intermolecular deubiquitination [21]. Li and colleagues performed screening and selected several DUBs to experiment with regulating their stability. Among these DUBs, the USP29 inactive mutant underwent ubiquitination-mediated proteasomal degradation, but WT USP29 ubiquitination was negligible, and the protein level remained higher than that of the inactive mutant form of USP29. Furthermore, USP29 formed a homomeric interaction through the N-terminal region and C-terminal catalytic domain, suggesting that USP29 with enzymatic activity inhibited its own ubiquitination through a homomeric interaction and thus prevented its degradation and maintained high protein levels [28]. We found that USP35 without activity (USP35CD) was degraded more rapidly than USP35 with activity (USP35CDC). In addition, high ubiquitination was observed only with USP35 inactive mutant form or the USP domain alone. Hence, we concluded that USP35 can deubiquitinate itself, which protects it from degradation induced by ubiquitination, and that this preventive effect is realized through a C-terminal domain-mediated homodimer interaction (Fig. 8).

DUBs whose stability is regulated by auto-deubiquitination can be targeted by E3 ligases and degraded by E3 ligase-mediated ubiquitination [29–31]. However, the E3 ligase involved in auto-regulatory deubiquitination has not been yet reported. In this study, we found that CHIP-mediated ubiquitination of USP35 induces its degradation. CHIP selectively ubiquitinates substrate captured by molecular chaperones, such as HSP90 [32]. We observed that HSP90 interacted with USP35 and that CHIP bound to HSP90 regulated the ubiquitination and degradation of USP35. Interestingly, WT USP35 or USP35 constructs, which showed full activity, was negligibly ubiquitinated by CHIP. On the basis of these results, we speculated that USP35 can cleave the ubiquitin chain attached to itself by CHIP and that this outcome depends on its own DUB activity (Fig. 8).

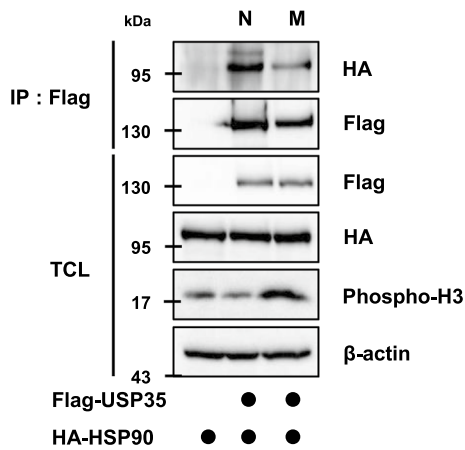
a



b



c



d

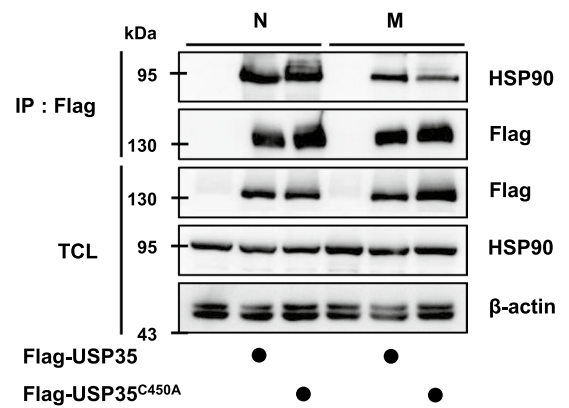


Fig. 7 The interaction between HSP90 and USP35 is decreased during mitosis. **a** HEK293T cells were cotransfected with HA-Aurora B and the indicated constructs of Flag-USP35. The interaction between HA-Aurora B and Flag-USP35 constructs was detected by immunoblotting after immunoprecipitation with an anti-Flag antibody. **b** HEK293T cells were transfected with HA-HSP90 or Myc-Aurora B alone, in combination with Flag-USP35, or altogether. The interaction between HSP90 or Aurora B and USP35 was detected by immunoblotting after immunoprecipitation with an anti-Flag antibody. **c, d** HeLa cells transfected with **(c)** Flag-USP35 and HA-HSP90 or **(d)** Flag-USP35 and Flag-USP35^{C450A} were synchronized in prometaphase by treatment with 100 ng/ml Nocodazol for 18 h. The interaction between HSP90 and USP35 was detected by immunoblotting after immunoprecipitation with **(c)** an anti-Flag antibody or **(d)** an anti-HSP90 antibody. N, normal cells (no synchronization); M, mitotic cells (synchronization)

As described above, both Aurora B and HSP90 bound to the same domain of USP35. To maintain the stability of Aurora B during mitosis [3], USP35 must not be degraded during this time. Therefore, the interaction of USP35 with HSP90 is attenuated during mitosis, leading to reduced ubiquitination of USP35 by CHIP. Indeed, the USP35 inactive mutant level increased in mitotic cells compared to normal cells, suggesting that CHIP-mediated degradation is decreased during mitosis (Fig. 7d).

Taken together, our work provides information on how the activity of USP35 is regulated by elucidating the role and structure of USP35 domains, and introduces a novel E3 ligase involved in the degradation of USP35. We believe that our study will contribute to a more accurate understanding of the cellular function of USP35.

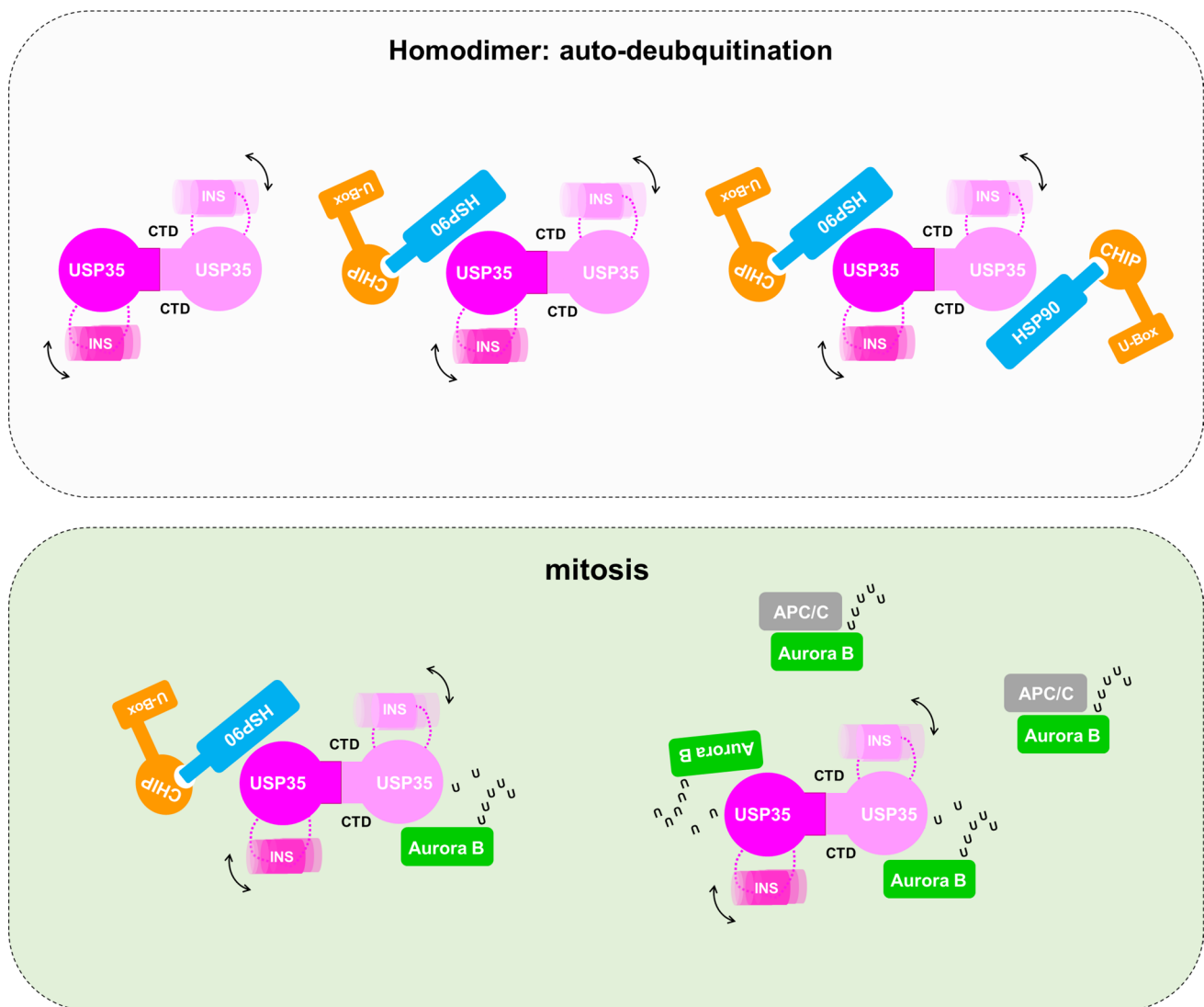


Fig. 8 Model showing auto-deubiquitination of the USP35 homodimer and its function during mitosis. WT USP35 forms a homodimer through the C-terminal domain. USP35 uses its own DUB activity to

cleave the ubiquitin chain attached by CHIP and thus prevents its own degradation. During mitosis, USP35 dissociates from HSP90 and then binds more Aurora B to deubiquitinate it

Supplementary Information The online version contains supplementary material available at <https://doi.org/10.1007/s00018-023-04740-9>.

Author contributions JP, EEK and EJS contributed to the study's conception and design. The most of experiments and analysis were performed by JP. SCS, KSJ, and MJL performed structural analysis and contributed to data collection. YK prepared materials and performed the cell analysis. The first draft of the manuscript was written by JP and SCS. EEK and EJS commented and approved the final manuscript, and conceived and supervised the study.

Funding This work was supported by a National Research Foundation of Korea (NRF) grants funded by the Korean government (MSIP) (2019R1A2C2004052, 2022R1A2C1092294) and Korea Institute of Science and Technology (KIST) Institutional Program (2E32312).

Data availability All relevant data are available from the corresponding authors upon reasonable request.

Declarations

Conflict of interest The authors declare that they have no conflict of interests.

References

- Wang Y, Serricchio M, Jauregui M, Shanbhag R, Stoltz T et al (2015) Deubiquitinating enzymes regulate PARK2-mediated mitophagy. *Autophagy* 11:595–606. <https://doi.org/10.1080/15548627.2015.1034408>
- Leznicki P, Natarajan J, Bader G, Spevak W, Schlattl A et al (2018) Expansion of DUB functionality generated by alternative isoforms—USP35, a case study. *J Cell Sci*. <https://doi.org/10.1242/jcs.212753>
- Park J, Kwon MS, Kim EE, Lee H, Song EJ (2018) USP35 regulates mitotic progression by modulating the stability of Aurora B. *Nat Commun* 9:688. <https://doi.org/10.1038/s41467-018-03107-0>
- Tsai IC, Adams KA, Tzeng JA, Shennib O, Tan PL et al (2019) Genome-wide suppressor screen identifies USP35/USP38 as therapeutic candidates for ciliopathies. *JCI Insight* 4:e130516. <https://doi.org/10.1172/jci.insight.130516>
- Cao J, Wu D, Wu G, Wang Y, Ren T et al (2021) USP35, regulated by estrogen and AKT, promotes breast tumorigenesis by stabilizing and enhancing transcriptional activity of estrogen receptor alpha. *Cell Death Dis* 12:619. <https://doi.org/10.1038/s41419-021-03904-4>
- Zhang J, Chen Y, Chen X, Zhang W, Zhao L et al (2021) Deubiquitinase USP35 restrains STING-mediated interferon signaling in ovarian cancer. *Cell Death Differ* 28:139–155. <https://doi.org/10.1038/s41418-020-0588-y>
- Wang W, Wang M, Xiao Y, Wang Y, Ma L et al (2022) USP35 mitigates endoplasmic reticulum stress-induced apoptosis by stabilizing RRBP1 in non-small cell lung cancer. *Mol Oncol* 16:1572–1590. <https://doi.org/10.1002/1878-0261.13112>
- Liu C, Chen Z, Ding X, Qiao Y, Li B (2022) Ubiquitin-specific protease 35 (USP35) mediates cisplatin-induced apoptosis by stabilizing BIRC3 in non-small cell lung cancer. *Lab Invest* 102:524–533. <https://doi.org/10.1038/s41374-021-00725-z>
- Tang Z, Jiang W, Mao M, Zhao J, Chen J et al (2021) Deubiquitinase USP35 modulates ferroptosis in lung cancer via targeting ferroportin. *Clin Transl Med* 11:e390. <https://doi.org/10.1002/ctm2.390>
- Faesen AC, Dirac AM, Shanmugham A, Ova H, Perrakis A et al (2011) Mechanism of USP7/HAUSP activation by its C-terminal ubiquitin-like domain and allosteric regulation by GMP-synthetase. *Mol Cell* 44:147–159. <https://doi.org/10.1016/j.molcel.2011.06.034>
- Clerici M, Luna-Vargas MP, Faesen AC, Sixma TK (2014) The DUSP-Ubl domain of USP4 enhances its catalytic efficiency by promoting ubiquitin exchange. *Nat Commun* 5:5399. <https://doi.org/10.1038/ncomms6399>
- Liu B, Sureda-Gomez M, Zhen Y, Amador V, Reverter D (2018) A quaternary tetramer assembly inhibits the deubiquitinating activity of USP25. *Nat Commun* 9:4973. <https://doi.org/10.1038/s41467-018-07510-5>
- Gersch M, Wagstaff JL, Toms AV, Graves B, Freund SMV et al (2019) Distinct USP25 and USP28 oligomerization states regulate deubiquitinating activity. *Mol Cell* 74:436–451 e437. <https://doi.org/10.1016/j.molcel.2019.02.030>
- Sauer F, Klemm T, Kollampally RB, Tessmer I, Nair RK et al (2019) Differential oligomerization of the deubiquitinases USP25 and USP28 regulates their activities. *Mol Cell* 74:421–435 e410. <https://doi.org/10.1016/j.molcel.2019.02.029>
- Das T, Shin SC, Song EJ, Kim EE (2020) Regulation of deubiquitinating enzymes by post-translational modifications. *Int J Mol Sci* 21:4028. <https://doi.org/10.3390/ijms21114028>
- Todi SV, Scaglione KM, Blount JR, Basrur V, Conlon KP et al (2010) Activity and cellular functions of the deubiquitinating enzyme and polyglutamine disease protein ataxin-3 are regulated by ubiquitination at lysine 117. *J Biol Chem* 285:39303–39313. <https://doi.org/10.1074/jbc.M110.181610>
- Meray RK, Lansbury PT Jr (2007) Reversible monoubiquitination regulates the Parkinson disease-associated ubiquitin hydrolase UCH-L1. *J Biol Chem* 282:10567–10575. <https://doi.org/10.1074/jbc.M611153200>
- Wijnhoven P, Konietzny R, Blackford AN, Travers J, Kessler BM et al (2015) USP4 auto-deubiquitylation promotes homologous recombination. *Mol Cell* 60:362–373. <https://doi.org/10.1016/j.molcel.2015.09.019>
- Mashtalir N, Daou S, Barbour H, Sen NN, Gagnon J et al (2014) Autodeubiquitination protects the tumor suppressor BAP1 from cytoplasmic sequestration mediated by the atypical ubiquitin ligase UBE2O. *Mol Cell* 54:392–406. <https://doi.org/10.1016/j.molcel.2014.03.002>
- Alonso-de Vega I, Martin Y, Smits VA (2014) USP7 controls Chk1 protein stability by direct deubiquitination. *Cell Cycle* 13:3921–3926. <https://doi.org/10.4161/15384101.2014.973324>
- Mei Y, Hahn AA, Hu S, Yang X (2011) The USP19 deubiquitinase regulates the stability of c-IAP1 and c-IAP2. *J Biol Chem* 286:35380–35387. <https://doi.org/10.1074/jbc.M111.282020>
- Svergun DI, Petoukhov MV, Koch MH (2001) Determination of domain structure of proteins from X-ray solution scattering. *Bioophys J* 80:2946–2953. [https://doi.org/10.1016/S0006-3495\(01\)76260-1](https://doi.org/10.1016/S0006-3495(01)76260-1)
- Kozin MB, Svergun DI (2001) Automated matching of high- and low-resolution structural models. *J Appl Crystallogr* 34:33–41. <https://doi.org/10.1107/S0021889800014126>
- Classen S, Hura GL, Holton JM, Rambo RP, Rodic I et al (2013) Implementation and performance of SIBYLS: a dual endstation small-angle X-ray scattering and macromolecular crystallography beamline at the Advanced Light Source. *J Appl Crystallogr* 46:1–13. <https://doi.org/10.1107/S0021889812048698>
- Connell P, Ballinger CA, Jiang J, Wu Y, Thompson LJ et al (2001) The co-chaperone CHIP regulates protein triage decisions mediated by heat-shock proteins. *Nat Cell Biol* 3:93–96. <https://doi.org/10.1038/35050618>
- Muller P, Ruckova E, Halada P, Coates PJ, Hrstka R et al (2013) C-terminal phosphorylation of Hsp70 and Hsp90 regulates

- alternate binding to co-chaperones CHIP and HOP to determine cellular protein folding/degradation balances. *Oncogene* 32:3101–3110. <https://doi.org/10.1038/onc.2012.314>
27. Grove TZ, Cortajarena AL, Regan L (2008) Ligand binding by repeat proteins: natural and designed. *Curr Opin Struct Biol* 18:507–515. <https://doi.org/10.1016/j.sbi.2008.05.008>
 28. Hou Z, Shi W, Feng J, Wang W, Zheng E et al (2021) Self-stabilizing regulation of deubiquitinating enzymes in an enzymatic activity-dependent manner. *Int J Biol Macromol* 181:1081–1091. <https://doi.org/10.1016/j.ijbiomac.2021.04.073>
 29. Huang X, Summers MK, Pham V, Lill JR, Liu J et al (2011) Deubiquitinase USP37 is activated by CDK2 to antagonize APC(CDH1) and promote S phase entry. *Mol Cell* 42:511–523. <https://doi.org/10.1016/j.molcel.2011.03.027>
 30. Bingol B, Tea JS, Phu L, Reichelt M, Bakalarski CE et al (2014) The mitochondrial deubiquitinase USP30 opposes parkin-mediated mitophagy. *Nature* 510:370–375. <https://doi.org/10.1038/nature13418>
 31. Chan NC, den Besten W, Sweredoski MJ, Hess S, Deshaies RJ et al (2014) Degradation of the deubiquitinating enzyme USP33 is mediated by p97 and the ubiquitin ligase HERC2. *J Biol Chem* 289:19789–19798. <https://doi.org/10.1074/jbc.M114.569392>
 32. Murata S, Minami Y, Minami M, Chiba T, Tanaka K (2001) CHIP is a chaperone-dependent E3 ligase that ubiquitylates unfolded protein. *EMBO Rep* 2:1133–1138. <https://doi.org/10.1093/embo-reports/kve246>

Publisher's Note Springer Nature remains neutral with regard to jurisdictional claims in published maps and institutional affiliations.

Springer Nature or its licensor (e.g. a society or other partner) holds exclusive rights to this article under a publishing agreement with the author(s) or other rightsholder(s); author self-archiving of the accepted manuscript version of this article is solely governed by the terms of such publishing agreement and applicable law.